Structure of effective catalyst layers around bubbles in a fluidized catalyst bed

doi: 10.1016/j.cej.2006.06.017

Structure of effective catalyst layers around bubbles in a fluidized catalyst bed

Chemical Engineering Journal 130 (2007) 119-124

Structure of effective catalyst layers around bubbles in a fluidized catalyst bed

Takami Kai[a*], Norihide Okada[a], Manabu Baba[a], Takeshige Takahashi[a], Masaki Misawa[b], Ion Tiseanu[c] and Naoki Ichikawa[b]

[a] *Department of Applied Chemistry and Chemical Engineering, Kagoshima University, Kagoshima 890-0065, Japan*
[b] *National Institute of Advanced Industrial Science and Technology, Tsukuba 305-8564, Japan*
[c] *National Institute for Lasers, Plasma and Radiation Physics, Bucharest-Magurele, Romania*

* Corresponding author.
Takami Kai

Department of Applied Chemistry and Chemical Engineering, Kagoshima University
1-21-40 Korimoto, Kagoshima 890-0065, Japan

Tel +81 99 285 8361; fax +81 285 8361. *E-mail address:* t.kai@cen.kagoshima-u.ac.jp (T. Kai).

Abstract

In a fluidized catalyst bed, the reactant gas transfers from the bubble phase to the emulsion phase and reactions proceed in the emulsion phase. The catalyst particles around the bubbles should contact the gases containing a high concentration of the reactants. Therefore, the effect of the catalysts around the bubbles is very important for estimating the conversion and selectivity in the reactor. In order to study the role of these catalysts, the hydrogenation of carbon dioxide was carried out in a fluidized catalyst bed. Based on the results, the amount of the catalyst that was effective for the reaction was calculated. In addition, the shape of the bubbles ascending in the fluidized catalyst bed was observed using a fast X-ray computer tomography (CT) scanner. The structure of the bubbles in the fluidized catalyst bed was very complicated and the surface area of the bubbles was much greater than the obtained when assuming spherical shaped bubble. By assuming that effective catalysts existed around the bubbles, the thickness of catalyst layer was obtained. Finally, the 3-dimensional images of the catalyst layers around the bubbles were reconstructed.

Keywords: Fluidization; Fluidized bed; Catalytic reaction; Reactor; Tomography; Bubble

1. Introduction

Fluidized catalyst beds have been used in chemical and refinery processes and extensively studied for more than 50 years. However, the features of this reactor are still not perfectly understood [1]. In a fluidized catalyst bed, since the reaction mainly occurs in the emulsion phase, the mass transfer rate between the bubbles and emulsion phase affects the overall reaction rate. Therefore, the bubble size, bubble shape, interface area and bubble ascending velocity are the important parameters for the design of a fluidized bed reactor.

Many reactor models have been proposed for fluidized catalyst beds. Almost all of these models considered the mass transfer between the bubble and emulsion phases. When the reaction rate becomes high and mass transfer is the rate determining step, conversion becomes independent of the reaction rate. However, some experimental results showed that the conversion increased with the reaction rate even when the reaction rate was very high. These results can be attributed to the region just above a distributor [2] and [3], the catalysts directly contacting with the bubble phase gas [3], [4], [5], [6] and[7], and the dilute phase above the dense phase [3], [4], [5], [6], [7], [8] and[9].

In the previously proposed reactor model, some mixing states in the emulsion phase have been assumed. However, the radial concentration distribution is not considered in these models. Based on the results of the direct observation of the bubbles and particle movements [10], there are many particles that seem to not directly contact the reactant gases. The lateral holdup of gas bubbles in a fluidized catalyst bed was almost parabolic [3]. The bubble frequency in the core part is high but it is lower near the wall. Since catalysts are porous materials, the mixing of the catalyst particles contribute to the transport of the gaseous components in the emulsion phase. The mixing of particles was enhanced by the passage of bubbles and the reactant gases were also well mixed in the core part of the bed. This effect is insignificant near the wall. When the reaction rates are high and the first order reaction rate $k=5\ s^{-1}$, 50 % of the reactants is converted to products within 0.14 s. In this case, the main components of the emulsion-phase gas near the wall are the products and the catalysts in this region are not effectively used for the reaction. On the other hand, the catalyst particles around the bubbles come in contact with the gas containing a high concentration of reactants. The reaction will almost completely proceed in this region when the reaction rate is much higher than the mass transfer rate between the two phases.

Therefore, the reactor model should consider the reaction rate, particle movement and bubble behavior. In the present study, the contact efficiency between the reactant gases and catalyst in a fluidized catalyst bed was investigated by carrying out the hydrogenation of carbon dioxide. Since the catalyst particles around the bubbles directly contact the reactants in the bubbles, they should contribute more to the reaction than the catalyst isolated from the bubbles. The amount of the effective catalyst was calculated from the reaction results based on some assumptions. In addition, an X-ray computer tomography (CT) scanner has been used for the analysis in the present study.

Grohse [11] has measured the variation in density of a bed using X-rays for the first time. Rowe and Partridge [12] observed the bubble shape by X-ray photographs and discussed the frequency of bubble splitting and coalescence. The studies on X-ray absorption have been conducted [13] and [14] by the group at University College London since this publication. X-ray computed tomography systems have been applied to determine

the local solid distribution in fluidized beds in the 1990s. Kantzas [15], [16] and [17] obtained images of the density and holdup using a fourth-generation modified medical scanner.

Recently, Kai et al. [18] and [19] have reconstructed 3-dimensional image of bubbles using a fast X-ray CT scanner. In the present study, the shape of the bubbles ascending in fluidized catalyst beds was observed using the X-ray CT scanner. Hence, the thickness of the effective catalyst layer could be obtained by using the surface area and the amount to effective catalyst. Finally, the 3-dimensional images of the bubbles and the effective catalyst layer were reconstructed.

2. Experimental

2.1 Hydrogenation of carbon dioxide

Two types of Ni-La_2O_3 / γ-Al_2O_3 catalysts were used. The mean particle diameter and the particle density of the catalyst were 54 μm and 660 kg m^{-3} for CAT-1 and 95 μm and 1090 kg m^{-3} for CAT-2, respectively. These catalysts were prepared by impregnating porous γ -Al_2O_3 with an aqueous solution of nickel nitrate. After being dried at 373 K, the impregnated powders were oxidized by air for 2 h at 523 K and reduced by hydrogen for 2 h at 623 K in a fluidized bed. **Fig. 1** shows the apparatus used for the fluidized bed reactor experiments. The reactor was made of stainless steel; the inner diameter was 3.0×10^{-2} m and the height was 1.5 m. The fraction of carbon dioxide in the feed gas was less than 4 % and the rest was hydrogen to avoid any influence by a decrease in the fluidization quality [20]. The superficial gas velocity was 0.075 and 0.15 m s^{-1}. The reaction temperature was varied from 413 to 623 K. The product gas was analyzed by a gas chromatograph. The reaction rate was analyzed in the fixed bed reactor having an inner diameter of 6.0×10^{-3} m.

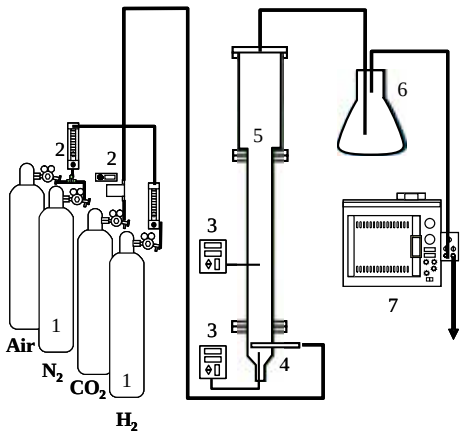

1. Gas cylinder
2. Flow meter
3. Temperature controller
4. Gas sparger
5. Fluidized bed reactor
6. Gas/Liquid separator
7. Gas chromatograph

Fig. 1. Fluidized bed reactor system.

2.2 CT measurements

A CT measurement was carried out for a fluidized bed with a 4.6×10^{-2} m diameter and 1.5 m long column made of a polyacrylic resin as shown in **Fig. 2**. Spherical silica-alumina particles with a broad particle size distribution were used as the fluidizing material. The mean particle size was 36 μm. The settled bed height was 0.86 m, and the height of the measuring plane was 0.6 m. Air from a high-pressure cylinder was used as the fluidizing gas.

The entire system consisted of an X-ray source, $CdWO_4$ scintillation detector arrays, a data acquisition system, controller unit, and image reconstruction system. Unlike conventional x-ray tubes, 18 electron guns were contained in a single vacuum chamber. Electrons emitted from the cathodes were accelerated up to 100 kV by a high voltage source. A single fan beam activated 32 detectors. A total of 122 detectors equally spaced at specific intervals were installed in a circle surrounding the measuring area. Since the interval of each scan was as high as 4 ms, the interface structure of the bubbles could be captured. The convolution-back projection method was employed for 2-dimensional imaging in a 129 × 129 pixel format. The reference scale of 5.0×10^{-2} m was digitized into 129, thus a single pixel matches 3.87×10^{-4} m in length for a 1.5×10^{-7} m^2 area. The details of the measuring system are described elsewhere [21] and [22].

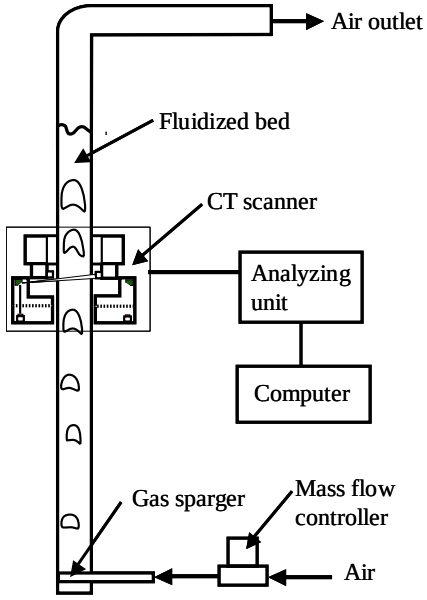

Fig. 2. Experimental equipment for the fast X-ray CT scanner / Fluidized bed assembly.

3. Results and discussion

3.1. Reaction analysis

The reaction rate equation obtained from the rate analysis in a fixed bed reactor was complicated. Since the molar fraction of hydrogen was excessive compared to the stoichiometric relation, a simplified equation was used by assuming a 1/3-order reaction with regard to CO_2 concentration:

$$-U_G \frac{dC_A}{dz} = k_{1/3} C_A^{1/3} \quad (1)$$

Fig. 3 shows the relation between the reaction temperature and conversion in the fluidized catalyst bed for CAT-1 and CAT-2. As the reaction temperature increased, the reaction rates became high and the conversion reached about 100 %. Generally, when the reaction rate becomes high in a fluidized catalyst bed, the mass transfer rate controls the overall reaction rate and the effect of the reaction rate on the conversion becomes low. However, the tendency shown in Fig. 3 disagrees with the general tendency. Since the superficial gas velocity in the present experiments was low, the effect of the dilute phase over the dense bed could be ignored.

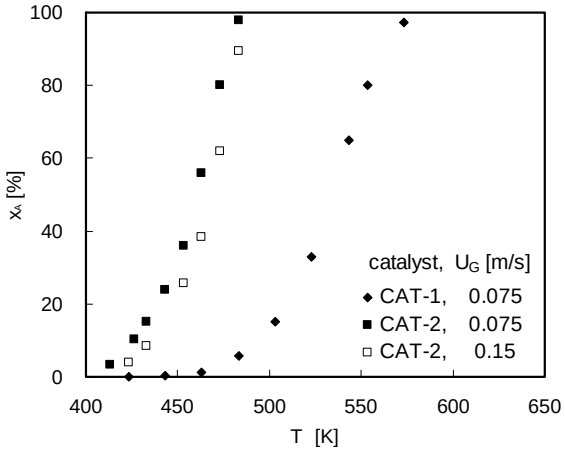

Fig. 3. The effect of reaction temperature on the conversion of carbon dioxide.

The dependence of the overall reaction rate on the temperature was examined. **Fig. 4** shows the Arrhenius plot of the reaction-rate constant obtained in the fixed bed. The result of the overall reaction-rate constant obtained in the fluidized bed is also shown in this figure. The rate constant in the fixed bed, $k_{1/3}$, is obtained by integrating Eq. (1):

$$k_{1/3} = \frac{3U_G C_A^{2/3}}{2L}\left[1-\left(1-x_A^{2/3}\right)\right] \tag{2}$$

The apparent reaction-rate constant, k_a, in the fluidized bed is calculated by the following equation:

$$k_a = \frac{3U_G C_A^{2/3}}{2L_q}\left[1-\left(1-x_A^{2/3}\right)\right] \tag{3}$$

The apparent activation energy was calculated to be 80 kJ mol^{-1} for both the fixed bed and fluidized bed from the slopes in Fig. 4. Consequently, the mass transfer between the bubble and emulsion phase was insignificant in this reaction system. The overall reaction rate was controlled mainly by the reaction rate. Hence, in this case, the role of the region just above a distributor and the direct contacting catalyst around the bubbles was significant. The important role of the catalyst contacting the bubble-phase gas has been emphasized [3] and [4]. These catalysts are called "direct contacting particles".

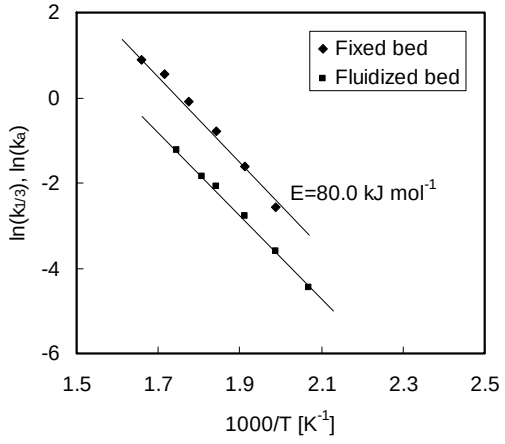

Fig. 4. Arrhenius plot of the overall reaction rate constant obtained in a fixed and fluidized bed reactors with CAT-1.

A stoichiometrically excess amount of hydrogen was supplied to the reactor and the concentration of hydrogen was kept at a high level in the upper part of the bed where the CO_2 conversion was high. Under this condition, the reaction rate was almost independent of the hydrogen concentration. Carbon dioxide should be transferred from the bubble phase to the emulsion phase and reacted with hydrogen to form methane. Since the overall reaction rate was strongly influenced by temperature, the reaction was probably catalyzed by the direct contacting particles when the reaction rate was high. The reactant gas in the bubble phase contacts the catalysts at the bubble surface, and the effect of the catalysts around the bubbles is significant. The role of the catalysts around the bubbles was investigated.

The amount of the direct contacting catalysts was calculated based on the experimental results. **Fig. 5** shows a comparison between the experimental conversion and the calculated conversion obtained from a plug-flow model considering the effective catalysts and ineffective catalysts. The fraction of the effective catalysts was determined by comparing the apparent reaction rate constant, k_a, with the reaction rate constant, $k_{1/3}$, obtained from the fixed bed reactor test. Therefore, the conversion in the fluidized bed is estimated by:

$$x_A = 1-\left(1-\frac{2\eta k_{1/3} L_q}{3U_G C_{A0}^{2/3}}\right)^{3/2} \tag{4}$$

where η is the mass fraction of the effective catalyst.

Fig. 5 indicates that the experimental results agreed very well with the calculated conversion obtained from the model. For the CAT-1 catalyst, the value of effective catalysts fraction was 25 % of all the catalysts in the bed when the superficial gas velocity was 0.075 m s^{-1}. For CAT-2, the fractions of the effective catalyst for the reaction were 13 % at the superficial gas velocity of 0.075 m s^{-1} and 17 % at 0.15 m s^{-1}.

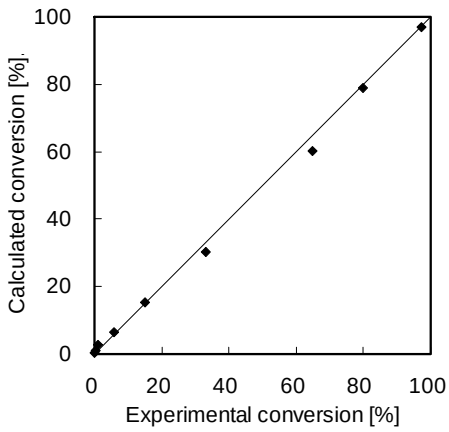

Fig. 5. The comparison of experimental conversion with the calculation from a model considering only direct contact catalysts.

3.2. Thickness of effective catalyst layer

Measurement of the area of the bubble interface was needed to estimate the thickness of the catalyst layer directly contacting the bubble-phase gas. The surface area of a bubble was obtained based on the 3-dimensional images of the bubbles as previously described [23]. **Fig. 6** shows the 3-dimensional images of a bubble ascending in the bed. The length of the horizontal square in the figure was 5.0×10^{-2} m. The vertical axis presents the elapsed time. If the bubble shape and ascending velocity do not change, the time axis is equivalent to the spatial coordinate. At this gas velocity, the bubble ascending velocity was calculated to be 0.33 m s^{-1} from the relation between the gas velocity and bed height. The bubble length in Fig. 6 was about 2.6×10^{-2} m. This

bubble image indicates that this bubble did not have a single spherical shape; the shape of the bubbles showed a complicated structure. This bubble is probably composed of several smaller bubbles [19].

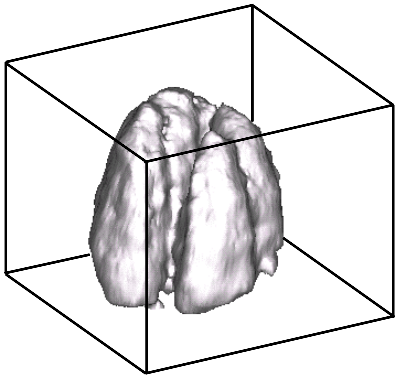

Fig. 6. Pseudo 3-dimensional image of a bubble.

Judging from the observation of the bubble structures in the present study, there are many catalyst particles in the interface between the bubbles and the emulsion phase. These particles contacted the gas in a bubble; therefore, they will correspond to the direct contacting particles. Beside the complicated structure of the bubbles, the bubbles rose in the bed with coalescence and splitting [10]. Therefore, the surface area becomes greater than that estimated on the basis of assuming a spherical shape [23].

The relationship between the thickness of the layer around a bubble and the volume of this layer was obtained when the diameter of a spherical bubble was 2.6×10^{-2} m. **Fig. 7** shows the ratio of the volume fraction of the catalyst layer, ε_c, to the bubble holdup, ε_b. When the thickness, δ, is 2×10^{-3} m, the value of ε_c is 54 % of that of ε_b for a spherically shaped bubble.

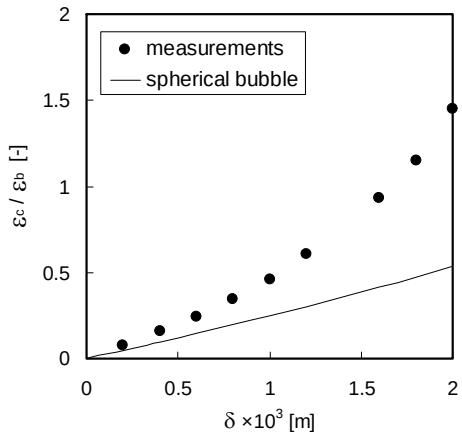

Fig. 7. Fraction of active layer around a bubble.

Although the bed density sharply changed at the bubble interface, the gray scale that corresponds to the transmission intensity of the X-rays gradually changed as shown in **Fig. 8**. The diameter of the circular image in Fig. 8 was 5.0×10^{-2} m. The thickness of the layer could be determined based on the intensity distribution. The relationship between the thickness and ε_b was obtained based on the bubble shape measured by the X-ray CT scanner. These results are also shown in Fig. 7. Since the shape of a real bubble is complicated as shown in Fig. 6, the ratio, $\varepsilon_c/\varepsilon_b$, was greater than that obtained from the assumption of a spherically shaped bubble. In this case, the fraction of the volume of effective catalyst layer was 54 % when δ is 1.1×10^{-3} m for the CAT-1 catalyst.

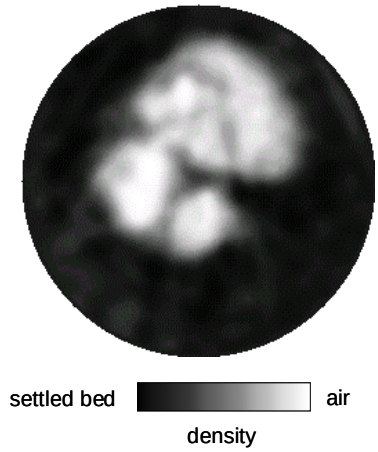

Fig. 8. Example of a slice of horizontal section images at measuring plane.

3.3. Three dimensional images of catalyst layer

Since the reactor was made of stainless steel and the bubble holdup could not be directly measured, it was measured in cold model experiments using CAT-1 particles. Consequently, the value of 0.1 was obtained when U_G was 0.075 m s^{-1}. As described above, in the case of CAT-1, the fraction of the effective catalysts around the bubbles was 25 %. Since the fraction of the emulsion phase was 0.9, the fraction of the effective emulsion of the aggregate bed was 0.225. The contacting efficiency just above the distributor is very high. Since the emulsion well mixed in this zone, not only the catalyst particles around the bubbles but also the other catalyst particles are effective for the reaction [2]. By assuming that the amount of the catalysts contained in this zone was 10 % of all the catalysts, the volume fraction of the effective catalyst around the bubbles was obtained to be 0.125. Therefore the ratio of ε_c to ε_b was 1.25. In this case, the thickness of the effective catalyst layer, δ, was 1.8×10^{-3} m from Fig. 7.

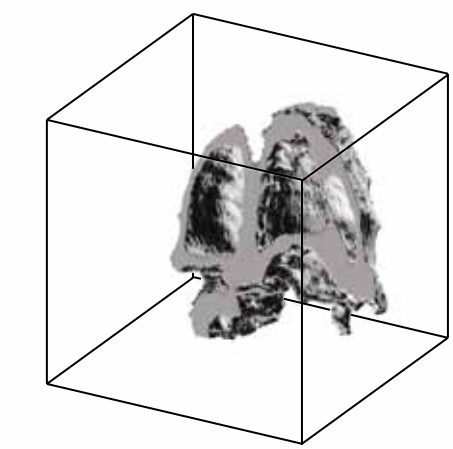

Fig. 9. Three-dimensional images of catalyst layer around bubble surface.

Finally, the 3-dimensional images of this catalyst layer around the bubbles were showed. **Fig. 9** shows the effective catalyst layer around bubbles vertically cut into two parts. The inside of one of the cut layer can be observed. In addition, an image was horizontally cut into two parts in the middle and **Fig. 10** shows the lower part of the cut image. The catalysts shown in these

figures will contact directly the bubble-phase gas. This layer was thin and the reaction mainly occurred in this layer when the reaction rate was high. These catalysts should be considered when the conversion and selectivity are predicted by the reactor models.

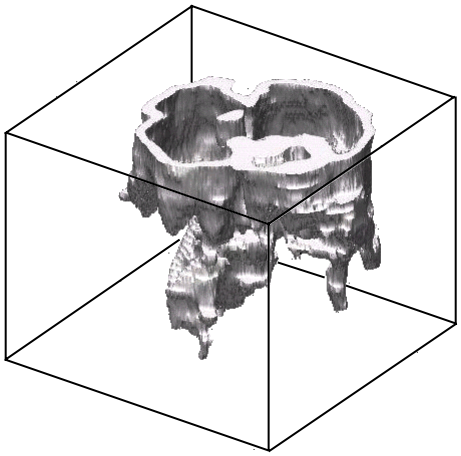

Fig. 10. Three-dimensional images of catalyst layer around bubble surface.

4. Conclusions

The hydrogenation of carbon dioxide was carried out in a fluidized catalyst bed. Since the activation energy of the apparent reaction-rate constant was almost the same as that obtained in a fixed bed reactor, the overall reaction rate in a fluidized catalyst bed was controlled by the reaction rate. The conversion in a fluidized catalyst bed was successfully estimated by the model assuming plug-flow contact and the effective catalyst in the bed. This catalyst probably contacted the bubble-phase gas in a layer around the bubble. The thickness of the layer was calculated to be 1.8×10^{-3} m by considering the distributor-zone catalyst as the other effective catalyst. In this calculation, the surface area was obtained from the 3-dimensional images of the bubbles measured by the X-ray CT scanner. Finally, the 3-dimensional images of the effective catalyst layer were successfully displayed.

Nomenclature

C_A	concentration of carbon dioxide (mol m^{-3})
C_{A0}	concentration of carbon dioxide in inlet gas (mol m^{-3})
E	activation energy (J mol^{-1})
$k_{1/3}$	reaction rate constant ($mol^{2/3}$ m^{-2} s^{-1})
k_a	apparent reaction rate constant in fluidized bed based on settled bed height ($mol^{2/3}$ m^{-2} s^{-1})
L	bed height of fixed bed reactor (m)
L_q	settled-bed height of fluidized bed (m)
T	reaction temperature (K)
U_G	superficial gas velocity (m s^{-1})
x_A	conversion of carbon dioxide
z	coordinate of bed height (m)

Greek letters

δ	thickness of effective catalyst layer around bubbles, m
ε_b	bubble holdup
ε_c	volume fraction of effective catalyst phase
η	mass fraction of effective catalyst

References

[1] D. Newton, M. Fiorentino, G.B. Smith, The Application of X-ray imaging to the developments of fluidized bed processes, Powder Technol. 120 (2002) 70-75.

[2] L. A. Behie, P. Kohoe, The grid region in a fluidized bed reactor, AIChE J. 19 (1976) 1070-1072.

[3] T. Miyauchi, S. Furusaki, S. Morooka, Y. Ikeda, Transport phenomena and reaction in fluidized catalyst beds, Advances in Chem. Eng. 11, Academic Press, New York, 1981, pp.275-448.

[4] T. Tsutsui, Consecutive reaction model considering direct contact in fluidized bed reactors, Kagaku Kogaku Ronbunshu 30 (2004) 249-255.

[5] N. Nozaki, S. Furusaki, T. Miyauchi, Determination of bed parameters by utilizing gas absorption for a fluidized catalyst bed of fine particles, Kagaku Kogaku Ronbunshu 10 (1984) 10-16.

[6] S. Furusaki, Y. Nozaki, K. Nakagiri, Mass transfer coefficients and amounts of direct-contact- catalyst in fluidized catalyst beds, Can. J. Chem. Eng. 62 (1984) 610-615.

[7] S. Furusaki, T. Kikuchi, T. Miyauchi, Axial distribution of reactivity inside a fluid-bed contactor, AIChE J. 22 (1976) 354-361.

[8] T. Kai, T. Tsutsui, S. Furusaki, Features of fluidized catalyst beds for proper design and operation of catalytic reactions, Ind. Eng. Chem. Res. 43 (2004) 5474 - 5482.

[9] H. I. De Lasa, J. R. Grace, The influence of the freeboard region in a fluidized bed catalytic cracking regenerator, AIChE J. 25 (1979) 984-991.

[10] T. Kai, T. Kanda, T. Takahashi, M. Kawaji, Application of photochromic dye to the measurement of particle movement in a fluidized bed, Powder Technol. 129 (2003) 22-29.

[11] E. W. Grohse, Analysis of gas-fluidized solid system by X-ray absorption," AIChE J. 1 (1955) 358-365.

[12] P. N. Rowe, B. A. Partridge, An X-ray study of bubbles in fluidised beds, Trans. Instn Chem. Engrs 43, (1965) 157-175.

[13] P. N. Rowe, D. J. Evertt, Fluidized bed bubbles viewed by X-rays, Part I - Experimental details and the interaction of bubbles with solid surfaces, Trans. Instn Chem. Engrs 50, (1972) 42-48.

[14] P. N. Rowe, L. Santoro, J. G. Yates, The devison of gas between bubble and interstitial phases in fluidized beds of fine powders, Chem. Eng. Sci. 33 (1978) 133-140.

[15] A. Kantzas, Computation of holdups in fluidized and trickle beds by computer-assisted tomography, AIChE J. 40 (1994), 1254-1261.

[16] A. Kantzas, I. Wright, N. Kalogerakis, Quantification of channeling in polyethylene resin fluid beds using X-ray computer assisted tomography (CAT), Chem. Eng. Sci. 52 (1997) 2023-2035.

[17] A. Kantzas, I. Wright, A. Bhargava, F. Li and K. Hamilton, Measurement of hydrodynamic data of gas-phase polymerization reactors using non-intrusive methods, Catal. Today 64 (2001) 189-203.

[18] T. Kai, T. Takahashi, M. Misawa, N. Ichikawa, I. Tiseanu, N. Takada, Application of fast X-ray CT Scanner to visualization of bubbles in fluidized bed, J. Chem. Eng. Japan, 33 (2000) 906-909.

[19] T. Kai, T. Takahashi, M. Misawa, N. Ichikawa, I. Tiseanu, Observation of 3-D structure of bubbles in a fluidized catalyst bed, Can. J. Chem. Eng. 83 (2005) 113-118.

[20] T. Kai, S. Furusaki, Methanation of carbon dioxide and fluidization quality in a fluid bed reactor - The influence of a decrease in gas volume. Chem. Eng. Sci. 42 (1987) 335-339.

[21] M. Misawa, N. Ichikawa, M. Akai, K. Hori, K. Tamura, G. Matsui, Development of fast X-ray CT system for transient two-phase flow measurement, Proceedings of the 6th Int. Conf. on Nucl. Eng., San Diego, USA, 1998, ICONE-6383.

[22] M. Misawa, N. Ichikawa, M. Akai, H. Monji, G. Matsui, Measurement of dynamic interface structure of slug flow in simplified rod bundles using a fast X-ray CT scanner, Proceedings of the 7th Int. Conf. on Nucl. Eng., Tokyo, Japan, 1999, ICONE-7099.

[23] T. Kanda, T. Kai, T. Takahashi, M. Misawa, N. Ichikawa, I. Tiseanu, Analysis of bubble in a three-dimensional fluidized catalyst bed using a fast X-ray CT scanner, Kagaku Kogaku Ronbunshu, 29 (2003) 112-117.